J. Plasma Physics (2006), *vol.* 72, *part* 3, *pp.* 329–339.
doi:10.1017/S0022377805004009 First published online 25 November 2005 Printed in the United Kingdom

Low-frequency responses in dusty plasmas

C. MARMOLINO[1] and U. DE ANGELIS[2]

[1]Dipartimento STAT, Università del Molise, Italy
[2]Dipartimento di Scienze Fisiche, Università di Napoli 'Federico II', Italy
(ciro.marmolino@unimol.it)

(Received 16 December 2004 and accepted 14 April 2005)

Abstract. In the parameter regime where the ion/electron–dust collisions dominate with respect to the plasma binary collisions, the presence of plasma fluxes to the dust surfaces and dust charge fluctuations can significantly modify the dusty plasma response to low-frequency perturbations, with respect to the multi-component response (no charging collisions, fixed dust charge). Here the response found from the kinetic theory which consistently takes into account collisions and charge fluctuations is examined, analytic expressions are given and the parameter regime where significant differences with respect to the multi-component approach arise is determined. The streaming instability is considered as a particular example and it is shown that both the real and imaginary parts of the frequency can be significantly changed with respect to the multi-component results.

1. Introduction

Owing to the charging collisions of electrons and ions with dust particles, dusty plasmas are dissipative systems and the dust charge fluctuates in response to fluctuating plasma currents. These effects have been consistently taken into account to find the plasma responses and dispersion relation (DR) in dusty plasmas [1–3], in the parameter regime $n_{\rm d}Z_{\rm d}^2/n_{\rm e} > 1$ ($n_{\rm d}$, $n_{\rm e}$ dust and electron densities, $q_{\rm eq} = -eZ_{\rm d}$ equilibrium dust charge, negative if only plasma currents contribute to the charging) where the electron/ion–dust collisions dominate with respect to the plasma binary collisions [4]. The charging collisions induce fluctuations of the dust charge which, in turn, induce plasma and field fluctuations, to be taken into account in the dusty plasma response [1, 2]. When all of these effects are negligible, the response (permittivity) is just the sum of the susceptibilities of the three components (electrons, ions and dust particles with fixed charge) [5]:

$$\varepsilon^{(0)}_{\mathbf{k},\omega} = 1 + \sum_{\alpha} \chi^{\alpha(0)}_{\mathbf{k},\omega}; \quad \chi^{\alpha(0)}_{\mathbf{k},\omega} = \frac{\omega^2_{{\rm p}\alpha}}{k^2} \int \frac{1}{\omega - \mathbf{k}\cdot\mathbf{v} + i0} \mathbf{k}\cdot\frac{\partial F^{\alpha}(\mathbf{v})}{\partial \mathbf{v}}\, d\mathbf{v} \tag{1.1}$$

where $\omega_{{\rm p}\alpha}$ and $F^{\alpha}(\mathbf{v})$ are the plasma frequency and equilibrium distribution function (normalized to 1) of the α-species ($\alpha = {\rm e}, {\rm i}, {\rm d}$) (the $i0$ in the denominator is the usual notation to account for causality). The charging collisions are described by cross sections $\sigma_{\alpha}(q, v)$ ($\alpha = {\rm e}, {\rm i}$; q is the dust charge, v is the electron or ion velocity, assumed to be much larger than the dust velocities) and collision frequencies

$$\nu_{{\rm d},\alpha}(v) = n_{\rm d} v \int \sigma_{\alpha}(q, v) F^{\rm d}(q, \mathbf{v}')\, dq\, d\mathbf{v}' \simeq v n_{\rm d} \sigma_{\alpha}(q_{\rm eq}, v) \tag{1.2}$$

where the last approximation assumes that the equilibrium distribution of dust charges $F^{\mathrm{d}}(q,\mathbf{v}')$ is peaked around $q = q_{\mathrm{eq}}$, the equilibrium value determined by the condition of zero net plasma flux to the dust surface, and the charge fluctuations are small ($|q-q_{\mathrm{eq}}|/|q_{\mathrm{eq}}| \ll 1$, see [6]). The approximate equality in (1.2) then comes from the zero order in the expansion of $\sigma_\alpha(q,v)$ around q_{eq} and the normalization condition:

$$\int F^{\mathrm{d}}(q,\mathbf{v}')\,dq\,d\mathbf{v}' = 1. \tag{1.3}$$

In the following estimates the orbital motion limited (OML) expressions for the cross sections will be used, for spherical grains of radius a:

$$\sigma_\alpha(q_{\mathrm{eq}},v) = \pi a^2\left(1-\frac{2q_{\mathrm{eq}}e_\alpha}{am_\alpha v^2}\right) \tag{1.4}$$

and for electrons it is $\sigma_{\mathrm{e}} = 0$ for $v < v_{\min} \equiv (2e^2Z_{\mathrm{d}}/am_{\mathrm{e}})^{1/2}$ (for negative dust particles).

Taking into account the charging collisions introduces changes in the electron and ion susceptibilities, which are given by [1, 2]

$$\chi^\alpha_{\mathbf{k},\omega} = \frac{\omega^2_{\mathrm{p}\alpha}}{k^2}\int \frac{1}{\omega-\mathbf{k}\cdot\mathbf{v}+i\nu_{\mathrm{d},\alpha}(v)}\mathbf{k}\cdot\frac{\partial F^\alpha(\mathbf{v})}{\partial\mathbf{v}}\,d\mathbf{v} \quad (\alpha = \mathrm{e},\mathrm{i}). \tag{1.5}$$

It should be stressed that in the presence of the dissipative collisions the equilibrium plasma distributions $F^\alpha(\mathbf{v})$ are not, in general, Maxwellian [7], although in the following estimates Maxwellian distributions will be assumed. The charging collisions and consequent dust charge fluctuations also introduce new 'mixed' terms in the dusty plasma response $\varepsilon_{\mathbf{k},\omega}$, such that it can no longer be written as the sum of the susceptibilities.

It is the aim of this work to discuss the dusty plasma permittivity (Sec. 2), to give analytical expressions for the low-frequency responses (see the Appendix), which can be useful in the study of low-frequency modes $\omega \ll kv_{T_{\mathrm{e}}}, kv_{T_{\mathrm{i}}}$ (where v_{T_α} is the thermal velocity) in dusty plasmas and to compare the behavior of the response with the multi-component case (Sec. 3) to find the parameter regime where significant differences appear and the effects of the charging collisions cannot be neglected. The case of relative dust–plasma streaming is considered as an example of the changes due to the effect of the charging collisions and dust charge fluctuations.

2. The permittivity of dusty plasmas

Neglecting the collisions with neutrals, the dusty plasma permittivity $\varepsilon_{\mathbf{k},\omega}$, derived in [3], contains plasma responses, dust responses and mixed dust–plasma responses. It can conveniently be written in the form

$$\varepsilon_{k,\omega} = 1+\chi^{\mathrm{e}}_{k,\omega}+\chi^{\mathrm{i}}_{k,\omega}+\chi^{\mathrm{d(eq)}}_{k,\omega}\left(1+\frac{\tilde{q}_{k,\omega}}{q_{\mathrm{eq}}}\right)+\frac{4\pi i}{k}\chi^{\mathrm{d,ch}}_{k,\omega}\beta_{k,\omega}(1+\tilde{\beta}_{k,\omega}). \tag{2.1}$$

The dust susceptibility $\chi^{\mathrm{d(eq)}}_{k,\omega}$ appearing in (2.1) is found to be given by (1.1) with ω_{pd} calculated with q_{eq} and the integrated dust distribution

$$F^{\mathrm{d}}(\mathbf{v}) = \int F^{\mathrm{d}}(q,\mathbf{v})\,dq. \tag{2.2}$$

https://doi.org/10.1017/S0022377805004009 Published online by Cambridge University Press

A new dust response present in (2.1) is the charging response:

$$\chi^{\mathrm{d,ch}}_{k,\omega} = in_{\mathrm{d}} \int \frac{F^{\mathrm{d}}(\mathbf{v})}{\omega - \mathbf{k}\cdot\mathbf{v} + i\nu_{\mathrm{ch}}}\, d\mathbf{v} \tag{2.3}$$

where ν_{ch} is the charging frequency, defined in [1]. The other 'mixed' responses appearing in (2.1) are strictly a consequence of the charging processes and they all vanish for $\sigma_\alpha = 0$; they are defined in [1,2] in general but here only their expressions in the particular case of low frequency Maxwellian equilibrium distributions and OML cross sections will be given. These responses depend on frequency through the expression $\omega - \mathbf{k}\cdot\mathbf{v}$, where $\mathbf{v}$ is the electron or ion velocity.

The kinetic equations for the evolution of the plasma and the dust distribution [1] contain collision integrals, for electron–dust, ion–dust and dust–dust collisions, in which the permittivity is evaluated at $\omega = \mathbf{k}\cdot\mathbf{v}'$ ($\mathbf{v}'$ dust velocity): $\varepsilon_{\mathbf{k},\mathbf{k}\cdot\mathbf{v}'}$. Therefore for thermal dust and plasma velocities $v_{\mathrm{d}}, v_{T_\alpha}$ such that $v_{\mathrm{d}} \ll v_{T_\alpha}$ and for low-frequency modes $\omega \simeq kv_{\mathrm{d}} \ll kv_{T_\alpha}$, the mixed responses can effectively be evaluated at zero frequency. In the same limit $\chi^{\mathrm{d,ch}}_{k,\omega} \simeq n_{\mathrm{d}}/\nu_{\mathrm{ch}}$ (for $\nu_{\mathrm{ch}} \gg \omega$) and, using the expression for $\beta_{k,\omega}$ as given in [1] the dusty plasma permittivity can be written as

$$\varepsilon_{k,\omega} = 1 + \chi^{\mathrm{e}}_{k,0} + \chi^{\mathrm{i}}_{k,0} + \chi^{\mathrm{d,e,i}}_{k,0} + \chi^{\mathrm{d(eq)}}_{k,\omega}\left(1 + \frac{\tilde{q}_{k,0}}{q_{\mathrm{eq}}} + \tilde{\chi}^{\mathrm{d,e,i}}_{k,0}\right) \tag{2.4}$$

where

$$\chi^{\mathrm{d,e,i}}_{k,0} \equiv \frac{4\pi i}{k}\frac{n_{\mathrm{d}}}{\nu_{\mathrm{ch}}}\frac{S_{k,0}}{1 - (n_{\mathrm{d}}/\nu_{\mathrm{ch}})\tilde{S}'_{k,0}}(1 + \tilde{\beta}_{k,0});$$

$$\tilde{\chi}^{\mathrm{d,e,i}}_{k,0} \equiv \frac{n_{\mathrm{d}}}{q_{\mathrm{eq}}\nu_{\mathrm{ch}}}\frac{\tilde{S}_{k,0}}{1 - (n_{\mathrm{d}}/\nu_{\mathrm{ch}})\tilde{S}'_{k,0}}(1 + \tilde{\beta}_{k,0}). \tag{2.5}$$

Notice that the only dependence of $\varepsilon_{k,\omega}$ on the frequency, in this regime, is through the dust equilibrium susceptibility $\chi^{\mathrm{d(eq)}}_{k,\omega}$. The zero-frequency responses, (2.4) and (2.5), have been calculated in [2] for Maxwellian distributions and OML cross sections and all depend on the parameters

$$z = \frac{e^2 Z_{\mathrm{d}}}{ak_{\mathrm{B}}T_{\mathrm{e}}}; \quad \tau = \frac{T_{\mathrm{i}}}{T_{\mathrm{e}}}; \quad P = \frac{n_{\mathrm{d}}Z_{\mathrm{d}}}{n_{\mathrm{e}}} \tag{2.6}$$

where T_{e} (T_{i}) is the electron (ion) temperature. The ion density n_{i} is always expressed through the quasi-neutrality condition $n_{\mathrm{i}} = n_{\mathrm{e}}(1 + P)$, for negative dust. They are reported here for convenience, using the same notation as in [2]:

$$\chi^{\alpha}_{k,0} = \chi^{\alpha(0)}_{k,0}[1 - G_\alpha(\kappa_\alpha)]; \quad (\alpha = \mathrm{e}, \mathrm{i}) \tag{2.7}$$

where $\chi^{\alpha(0)}_{k,0} = (k^2 d_\alpha^2)^{-1}$ are the zero-frequency susceptibilities from (1) and $d_\alpha = v_{T_\alpha}/\omega_{\mathrm{p}\alpha}$ is the electron or ion Debye length;

$$S_{k,0} = -\frac{i\nu_{\mathrm{ch}}}{\pi a\kappa_{\mathrm{e}}n_{\mathrm{d}}}\frac{1}{1 + \tau + z}\left\{(\tau + z)[1 - F_{\mathrm{e}}(\kappa_{\mathrm{e}})] + \frac{\kappa_{\mathrm{e}}}{\kappa_{\mathrm{i}}}\left[1 + \frac{\tau}{z} - F_{\mathrm{i}}(\kappa_{\mathrm{i}})\right]\right\} \tag{2.8}$$

$$\tilde{S}_{k,0} = -\frac{q_{\mathrm{eq}}\nu_{\mathrm{ch}}}{n_{\mathrm{d}}}\frac{1}{1 + \tau + z}\left\{\left(1 + \frac{\tau}{z}\right)F_{\mathrm{e}}(\kappa_{\mathrm{e}}) - F_{\mathrm{i}}(\kappa_{\mathrm{i}})\right\} \tag{2.9}$$

https://doi.org/10.1017/S0022377805004009 Published online by Cambridge University Press

$$\tilde{S}'_{k,0} = \frac{\nu_{\rm ch}}{n_{\rm d}} \frac{1}{1+\tau+z} \left\{ (\tau+z) F_{\rm e}^{M}(\kappa_{\rm e}) + F_{\rm i}^{M}(\kappa_{\rm i}) \right\} \tag{2.10}$$

$$\tilde{q}_{k,0} = \frac{q_{\rm eq}}{P} \{ G_{\rm e}(\kappa_{\rm e}) - (1+P) G_{\rm i}(\kappa_{\rm i}) \} \tag{2.11}$$

$$\tilde{\beta}_{k,0} = P(z+\tau) \frac{v_{T\rm i} z}{v_{T\rm e} \tau} G_{\rm e}^{M}(\kappa_{\rm e}) + P G_{\rm i}^{M}(\kappa_{\rm i}) \tag{2.12}$$

where the dimensionless wavenumbers are defined as

$$\kappa_{\rm e} = \frac{k}{\pi a^2 n_{\rm d}}, \quad \kappa_{\rm i} = \kappa_{\rm e} \frac{\tau}{z} \tag{2.13}$$

and all the functions $G_{\rm e}$, $G_{\rm i}$, $F_{\rm e}$, $F_{\rm i}$, $G_{\rm e}^{M}$, $G_{\rm i}^{M}$, $F_{\rm e}^{M}$ and $F_{\rm i}^{M}$ are given in [2] in a form ready for numerical calculation, while their analytical expansions, for large and small $\kappa_{\rm e}$, are given here in the Appendix. These expansions are particularly useful in the ranges where the numerical errors become of the same order of magnitude as the functions. The charging frequency, defined in [1], has the following approximate expression in the OML approximation:

$$\nu_{\rm ch} \approx \omega_{\rm pi} \frac{a}{\sqrt{2\pi} d_{\rm i}} (1+\tau+z). \tag{2.14}$$

Using the expressions (2.7)–(2.12) in (2.4) the low-frequency permittivity can finally be written in the form

$$\varepsilon_{k,\omega} = 1 + \chi_{k,\omega}^{(0)} + \delta\chi_{k,\omega}^{\rm coll}(P,z,\tau) \tag{2.15}$$

where $\chi_{k,\omega}^{(0)} = \chi_{k,0}^{\rm e(0)} + \chi_{k,0}^{\rm i(0)} + \chi_{k,\omega}^{\rm d(eq)}$ is the multi-component result and the correction due to the effects of charging collisions is given by

$$\delta\chi_{k,\omega}^{\rm coll}(P,z,\tau) = A_k + \chi_{k,\omega}^{\rm d(eq)} B_k \tag{2.16}$$

with

$$A_k = -\chi_{k,0}^{\rm e(0)} G_{\rm e} - \chi_{k,0}^{\rm i(0)} G_{\rm i} + \frac{4}{\pi a^3 n_{\rm d} \kappa_{\rm e}^2} \left[1+\tau+z-(\tau+z)F_{\rm e} - \frac{z}{\tau}(F_{\rm i}-1) \right] R_k \tag{2.17}$$

$$B_k = \frac{1}{P} G_{\rm e} - \frac{1+P}{P} G_{\rm i} + \left(F_{\rm i} - \frac{\tau+z}{z} F_{\rm e} \right) R_k \tag{2.18}$$

and

$$R_k \equiv \frac{1 + P(\tau+z)(v_{T_{\rm i}}/v_{T_{\rm e}})(z/\tau) G_{\rm e}^{M} + P G_{\rm i}^{M}}{1+\tau+z-(\tau+z)F_{\rm e}^{M} - F_{\rm i}^{M}}. \tag{2.19}$$

3. Numerical results

The difference between the multi-component result and the result including the effects of the charging collisions depends on the parameters P, z and τ (they are not independent if a charging equation is included) and on the frequency in the dust susceptibility. For a Maxwellian dust distribution this is given by

$$\chi_{k,\omega}^{\rm d(eq)} = \frac{\omega_{\rm pd}^2}{k^2 v_{T\rm d}^2} \left(1 - 2y e^{-y^2} \int_0^y e^{t^2}\, dt \right) \tag{3.1}$$

https://doi.org/10.1017/S0022377805004009 Published online by Cambridge University Press

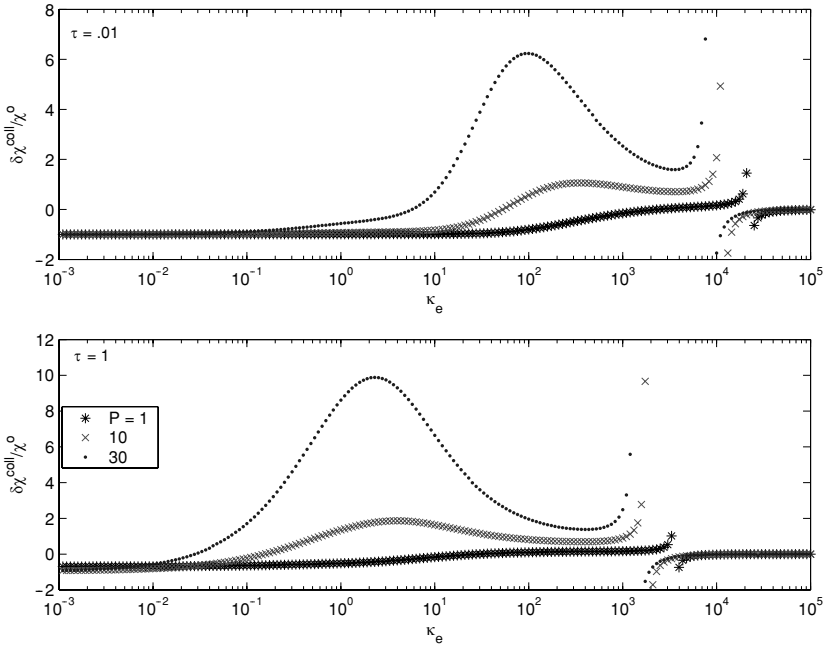

Figure 1. The relative difference in the susceptibility between the dusty and the multi-component results, as a function of the dimensionless wavenumber κ_e, for two values of τ and different values of P. The discontinuity, visible for large κ_e, is discussed in the text.

with $y = \omega/(\sqrt{2}kv_{Td})$. As an estimate, the difference is shown at a frequency $\omega = \omega_{pd}$, which is representative of most of the low-frequency dusty plasma modes. A calculation for a particular mode is given at the end of this section. The dust Debye radius can be written as

$$\frac{v_{Td}^2}{\omega_{pd}^2} = d_d^2 = d_i^2 \frac{1+P}{P} \frac{T_d}{T_i Z_d} = d_i^2 \frac{n_d}{n_e} \frac{1+P}{P^2} \tag{3.2}$$

where the last equality is for $T_d \simeq T_i$. The ratio of dust to electron density is therefore an additional parameter. Figure 1 shows the relative difference in the susceptibility $\delta\chi^{coll}/\chi^{(0)}$ as a function of κ_e, for $T_e = 10^4$ K and of the ratio $a/\Delta = 10^{-2}$ between the grain radius and the inter-dust particle distance, two values of τ and different values of P, with z calculated as a function of P and τ from the orbit limited motion equation for grain charging. Notice that, for small κ_e, both $\delta\chi^{coll}$ and $\chi^{(0)}$ go as $1/\kappa_e^2$ with opposite sign so that their ratio goes to -1, corresponding to $\varepsilon_{\kappa,\omega} \to 1$ at small κ_e, quite different from the behavior of $\varepsilon^{(0)}_{\kappa,\omega} = 1 + \chi^{(0)}_{\kappa,\omega}$. For large κ_e, $\delta\chi^{coll}$ goes to zero as $1/\kappa_e$, while $\chi^{(0)}$ reduces to $\chi^{d}_{\kappa,\omega}$ which is -1, then their ratio goes to zero as $1/\kappa_e$ and $\varepsilon_{\kappa,\omega} \to \varepsilon^{(0)}_{\kappa,\omega}$. This behavior also explains the discontinuity visible in the figure at large κ_e. In fact, the discontinuity is located at $\chi^{(0)} = 0$, i.e. essentially at $\chi^{i(0)}_{\kappa,0} \simeq 1$ or $\kappa_e^2 \simeq 4\zeta(1+P)/(\pi a^3 n_d P)$. The difference between the two approaches is negligible only for very large values of κ_e.

https://doi.org/10.1017/S0022377805004009 Published online by Cambridge University Press

Finally, as an example of the effect on the real and imaginary parts of the frequency of a particular mode, the case of streaming dust (with velocity $\mathbf{v}_0$ with respect to the plasma) is considered. Taking the dust susceptibility as

$$\chi_{k,\omega}^{\mathrm{d(eq)}} = \frac{\omega_{\mathrm{pd}}^2}{\Omega^2}; \quad \Omega = \omega - \mathbf{k}\cdot\mathbf{v}_0 \tag{3.3}$$

and defining

$$a_{k,0} = 1 + \chi_{k,0}^{\mathrm{e}(0)} + \chi_{k,0}^{\mathrm{i}(0)} \tag{3.4}$$

$$a_k = 1 + \chi_{k,0}^{\mathrm{e}} + \chi_{k,0}^{\mathrm{i}} + \chi_{k,0}^{\mathrm{d,e,i}} \tag{3.5}$$

$$b_k = 1 + \frac{\tilde{q}_{k,0}}{q_{\mathrm{eq}}} + \tilde{\chi}_{k,0}^{\mathrm{d,e,i}} \tag{3.6}$$

the solution of the dispersion relation is given by

$$\Omega^2 = -\omega_{\mathrm{pd}}^2 \frac{b_k}{a_k}. \tag{3.7}$$

In the multi-component case ($b_k = 1, a_k = a_{k,0} > 0$) the solution for the complex frequency $\omega = \omega_{\mathrm{r}}^0 + i\omega_{\mathrm{i}}^0$ is

$$\omega = \mathbf{k}\cdot\mathbf{v}_0 + i\frac{\omega_{\mathrm{pd}}}{\sqrt{a_{k,0}}}. \tag{3.8}$$

In the general case the solutions depend on the sign of b_k/a_k (which can change depending on the parameter regime). For $b_k/a_k > 0$ it is

$$\omega = \mathbf{k}\cdot\mathbf{v}_0 + i\omega_{\mathrm{pd}}\sqrt{\frac{b_k}{a_k}} \tag{3.9}$$

while for $b_k/a_k < 0$ the solution is real (no instability):

$$\omega_{\mathrm{r}} = \mathbf{k}\cdot\mathbf{v}_0 + \omega_{\mathrm{pd}}\sqrt{\frac{-b_k}{a_k}}. \tag{3.10}$$

The relative differences between the imaginary parts and the real parts are shown in Fig. 2 for several values of the parameters. Again, it is clear that the dusty mode can be very different from the multi-component one. In particular, the largest differences are in the imaginary part of the solution for $P > 1$, while they appear in the real part of the solution for $P < 1$, whatever the values of τ. The variations, both in the imaginary and real parts, depend strongly on τ, the dusty solution becoming almost an order of magnitude more instable for $\tau = 0.01$ and large P, while the instability is reduced with respect to the multi-component solution for $\tau = 1$ for all the P values we investigated.

4. Conclusions

The charging collisions of plasma particles with dust and the dust charge fluctuations can modify the dusty plasma response and low-frequency dusty plasma modes in a substantial way, compared with the response of multi-component theory which neglects the charging collisions and considers a fixed dust charge. The effects are summarized in (2.15) as a change in the plasma susceptibilities and are shown

https://doi.org/10.1017/S0022377805004009 Published online by Cambridge University Press

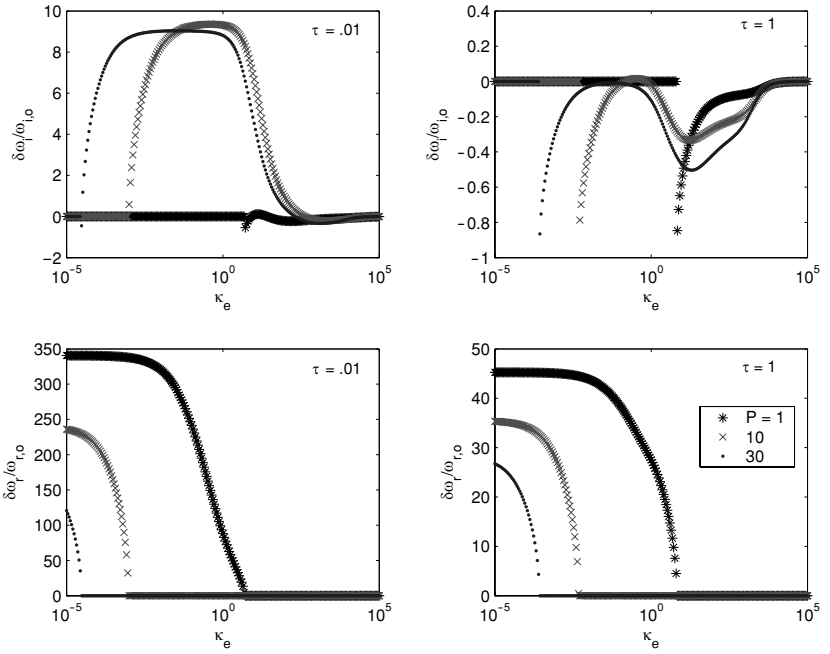

Figure 2. The relative difference in the imaginary parts $\delta\omega_{\rm i}/\omega_{\rm i}^0 = \sqrt{a_{k,0}b_k/a_k} - 1$ (top panels) and in the real parts $\delta\omega_{\rm r}/\omega_{\rm r}^0 = \omega_{\rm pd}\sqrt{-b_k/a_k}/\mathbf{k}\cdot\mathbf{v}_0$ (bottom panels) of the solution of the dispersion relation between the dusty and the multi-component results, versus the dimensionless wavenumber $\kappa_{\rm e}$, for two values of τ and different values of P. The relative difference in the real parts has been evaluated for a streaming velocity $\mathbf{v}_0$ of the order of the thermal dusty speed, $v_{T\,\rm d}$.

in Fig. 1 for several values of parameters. The effect is particularly enhanced for larger values of the density parameter P.

The particular example of drift instability shows differences (with respect to the multi-component theory) not only in the phase velocity (it can be orders of magnitude) but notably in the imaginary part of the frequency which can be smaller (reduced instability) or larger (enhanced instability) than the multi-component (MC) result depending on the ion to electron temperature ratio.

Acknowledgement

Work supported by the European Union 'Human Potential–Research Training Network', Grant No HPRN-CT2000-00140.

Appendix. Analytical expansions

The correction to the multi-component result is given in terms of the functions $G_{\rm e}$, $G_{\rm i}$, $F_{\rm e}$, $F_{\rm i}$, $G_{\rm e}^M$, $G_{\rm i}^M$, $F_{\rm e}^M$ and $F_{\rm i}^M$ defined in [2]. Here we give analytical expansions for them expressing both the electronic and ionic functions in terms of the electronic dimensionless wavenumber, $\kappa_{\rm e}$, and of the parameters z and $\zeta = z/\tau$, respectively. The analytical expansions are very accurate in the following ranges

Table A.1. Coefficients for the expansions of G_e and G_e^M for $\kappa_e < \min[\frac{1}{2}, 1/(1+z)]$.

	$G_e(\kappa_e)$	$G_e^M(\kappa_e)$
$f_{e0}(z)$	$2e^{-z}\sqrt{\frac{z}{\pi}} + \operatorname{erfc}(\sqrt{z})$	$\frac{2e^{-z}}{\sqrt{\pi}}\left\{\sqrt{z}\left(\frac{\pi}{2}-\frac{2}{3}\right) + \frac{4z-1}{8z\sqrt{z}} - \sqrt{z}[C+\ln(z)+E_1(z)] + \sqrt{\pi}\operatorname{erfc}(\sqrt{z})\left(1-z-\frac{z^2}{6}\right) + \frac{\sqrt{z}e^{-z}}{2}\left(\frac{11}{6}+\frac{z}{3}-\frac{3}{4z}+\frac{1}{4z^2}\right)\right\}$
$f_{e1}(z)$	0	$-2\sqrt{\frac{z}{\pi}}e^{-z}$
$f_{e2}(z)$	$2ze^{-z}\sqrt{\frac{z}{\pi}}\left(\frac{\pi}{4}-\frac{5}{3}\right)$	$2\sqrt{\frac{z}{\pi}}e^{-z}\left(3-2z\right)\left(\frac{\pi}{8}-\frac{5}{6}\right)$
$f_{e3}(z)$	0	0
$f_{e4}(z)$	$e^{-z}\operatorname{erfc}(\sqrt{z})\left(\frac{5z^2}{2}-\frac{5z}{3}-\frac{1}{3}\right) + \frac{\sqrt{z}e^{-z}}{12\sqrt{\pi}}\{(-15+7e^{-z}) + 20[\ln z + C + E_1(z)]z + (10\pi - 37 - 22e^{-z})z + [26-4\pi-8E_1(z)]z^2 - 8(C+\ln z)z^2\}$	$\frac{2e^{-z}}{\sqrt{\pi}}\left\{\sqrt{z}(15-20z+4z^2)\left(\frac{\pi}{48}-\frac{3}{32}\right) + \frac{\sqrt{z}}{12}(8+6z-3z^2) - \frac{\sqrt{z}e^{-z}}{3}\left(\frac{13}{4}-2z\right) - \frac{\sqrt{\pi}}{6}\operatorname{erfc}(\sqrt{z})(2-10z+5z^2) + \frac{\sqrt{z}}{24}(4z^2-20z+15)[C+\ln(z)+E_1(z)]\right\}$
$f_{e5}(z)$	$\frac{2ze^{-z}}{3}\sqrt{\frac{z}{\pi}}\left(\frac{5}{2}-z\right)$	$\sqrt{\frac{z}{\pi}}\frac{e^{-z}}{12}(15-20z+4z^2)$

of κ_e:

$$f_e(\kappa_e, z) = \begin{cases} f_{e0}(z) + f_{e1}(z)\ln\kappa_e + f_{e2}(z)\kappa_e & \\ +f_{e3}(z)\kappa_e\ln\kappa_e + f_{e4}(z)\kappa_e^2 + f_{e5}(z)\kappa_e^2\ln\kappa_e & \left(\kappa_e < \min\left[\frac{1}{2}, \frac{1}{(1+z)}\right]\right) \\ \frac{F_{e1}}{\kappa_e} + \frac{F_{e2}}{\kappa_e^2} & (\kappa_e > 1) \end{cases} \tag{A 1}$$

$(f_e \equiv G_e, G_e^M, F_e, F_e^M)$

$$f_i(\kappa_e, \zeta) = \begin{cases} f_{i0}(\zeta) + f_{i2}(\zeta)\kappa_e^2 & (\kappa_e < 1) \\ \frac{G_{i1}(\zeta)}{\kappa_e} + \frac{G_{i2}(\zeta)}{\kappa_e\sqrt{\kappa_e}} + \frac{G_{i3}(\zeta)}{\kappa_e^2} + \frac{G_{i4}(\zeta)}{\kappa_e^2\sqrt{\kappa_e}} & (\kappa_e > \max[2, 1+\zeta]) \\ \frac{F_{i1}(\zeta)}{\kappa_e} + \frac{F_{i2}(\zeta)}{\kappa_e}\ln\kappa_e + \frac{F_{i3}(\zeta)}{\kappa_e^2} + \frac{F_{i4}(\zeta)}{\kappa_e^2}\ln\kappa_e & (\kappa_e > \max[2, 1+\zeta]) \end{cases} \tag{A 2}$$

$(f_i \equiv G_i, G_i^M, F_i, F_i^M)$.

https://doi.org/10.1017/S0022377805004009 Published online by Cambridge University Press

Table A.2. Coefficients for the expansions of F_e and F_e^M for $\kappa_e < \min[\frac{1}{2}, 1/(1+z)]$.

	$F_e(\kappa_e)$	$F_e^M(\kappa_e)$
$f_{e0}(z)$	1	1
$f_{e1}(z)$	0	0
$f_{e2}(z)$	0	$z\left(\frac{\pi}{4}-\frac{5}{3}\right)$
$f_{e3}(z)$	0	0
f_{e4}	$z^2\left(\frac{\pi}{6}-\frac{3}{4}\right) - \frac{[1+2z-z^2(C+\ln z)]}{3}$	$-\frac{1}{3}+\left(\frac{\pi}{3}-\frac{7}{6}\right)z+\left(\frac{13}{12}-\frac{\pi}{6}\right)z^2 + \frac{z(2-z)(C+\ln z)}{3}$
$f_{e5}(z)$	$\frac{z^2}{3}$	$\frac{z(2-z)}{3}$

Table A.3. Coefficients of the expansions of the electronic functions for $\kappa_e > 1$.

	$F_{e1}(z)$	$F_{e2}(z)$
$G_e(\kappa_e)$	$\sqrt{\pi z}e^{-z} + \pi\left(\frac{1}{2}-z\right)\operatorname{erfc}(\sqrt{z})$	$-2e^{-z}\sqrt{\frac{z}{\pi}}(1+2z) - (1-4z-4z^2)\operatorname{erfc}(\sqrt{z})$
$G_e^M(\kappa_e)$	$\pi\operatorname{erfc}(\sqrt{z})$	$4\sqrt{\frac{z}{\pi}}e^{-z} - (2+4z)\operatorname{erfc}(\sqrt{z})$
$F_e(\kappa_e)$	$\frac{\pi}{2}[1-z+z^2e^z E_1(z)]$	$-1+2z+z^2-z^2e^z(3+z)E_1(z)$
$F_e^M(\kappa_e)$	$\frac{\pi}{2}[1-ze^z E_1(z)]$	$-1-z+ze^z(2+z)E_1(z)$

Table A.4. Coefficients of the expansions of the ionic functions for $\kappa_e < 1$.

	$f_{i0}(\zeta)$	$f_{i2}(\zeta)$
$G_i(\kappa_e)$	1	$\frac{2\zeta}{3}\left[\left(2-\frac{1}{2\zeta}+\zeta\right) - \sqrt{\pi\zeta}e^{\zeta}\operatorname{erfc}(\sqrt{\zeta})\left(\frac{5}{2}+\zeta\right)\right]$
$G_i^M(\kappa_e)$	$2\zeta[1-\sqrt{\pi\zeta}e^{\zeta}\operatorname{erfc}(\sqrt{\zeta})]$	$-\frac{2\zeta}{3}\left[\left(1+\frac{9\zeta}{4}+\frac{\zeta^2}{2}\right) - \sqrt{\pi\zeta}e^{\zeta}\operatorname{erfc}(\sqrt{\zeta})\left(\frac{15}{8}+\frac{5\zeta}{2}+\frac{\zeta^2}{2}\right)\right]$
$F_i(\kappa_e)$	$\frac{1+\zeta}{\zeta}$	$-\frac{1}{3}\left[\frac{1-\zeta}{\zeta}+\zeta e^{\zeta}E_1(\zeta)\right]$
$F_i^M(\kappa_e)$	1	$-\frac{1+\zeta-\zeta(2+\zeta)e^{\zeta}E_1(\zeta)}{3}$

The explicit expressions of all the coefficients are given in Tables A.1–A.6. The results are shown in Figs A.1 and A.2 where the expressions are compared to the results of numerical calculations of the functions for their expressions in [2]. As the figures show the analytic expressions provide an excellent representation of

https://doi.org/10.1017/S0022377805004009 Published online by Cambridge University Press

Table A.5. Coefficients of the expansions of the ionic functions $G_{\rm i}$ for $\kappa_{\rm e} > \max[2, 1+\zeta]$.

	$G_{\rm i}(\kappa_{\rm e})$	$G_{\rm i}^M(\kappa_{\rm e})$
$G_{\rm i1}(\zeta)$	$\pi\left(\zeta+\frac{1}{2}\right)$	$\pi\zeta$
$G_{\rm i2}(\zeta)$	$-\dfrac{2\zeta^{3/2}}{\sqrt{\pi}}\left(\pi+\dfrac{10}{7}\right)$	$-\dfrac{2\zeta\sqrt{\zeta}}{7\sqrt{\pi}}(10+7\pi)$
$G_{\rm i3}(\zeta)$	$(4\zeta^2-4\zeta-1)$	$2\zeta(2\zeta-1)$
$G_{\rm i4}(\zeta)$	$\dfrac{2\zeta^{3/2}}{3\sqrt{\pi}}\left[\left(\dfrac{157}{9}-\dfrac{5\pi}{2}\right)-\zeta\left(\dfrac{314}{45}-\pi\right)\right]$	$\dfrac{\zeta^{3/2}}{3\sqrt{\pi}}(3-2\zeta)\left(\dfrac{314}{45}-\pi\right)$

Table A.6. Coefficients of the expansions of the ionic functions $F_{\rm i}$ for $\kappa_{\rm e} > \max[2, 1+\zeta]$.

	$F_{\rm i}(\kappa_{\rm e})$	$F_{\rm i}^M(\kappa_{\rm e})$
$F_{\rm i1}(\zeta)$	$\dfrac{\pi\zeta}{2}\left[\dfrac{1+2\zeta}{\zeta^2}-C-\ln\zeta\right]-\dfrac{\zeta}{9}$	$\dfrac{\pi\zeta}{2}\left[\dfrac{1}{\zeta}-C-\ln\zeta\right]-\dfrac{\zeta}{9}$
$F_{\rm i2}(\zeta)$	$-\dfrac{\pi\zeta}{2}$	$-\dfrac{\pi\zeta}{2}$
$F_{\rm i3}(\zeta)$	$\zeta(3-\zeta)\left[\dfrac{5}{12}-\dfrac{\pi}{2}+C+\ln\zeta\right]$ $+\zeta^2+\zeta-\dfrac{1+3\zeta}{\zeta}$	$\zeta\left(1-\dfrac{\zeta}{2}\right)\left[\dfrac{5}{6}-\pi+2(C+\ln\zeta)\right]$ $+\zeta^2+\zeta-1$
$F_{\rm i4}(\zeta)$	$\zeta(3-\zeta)$	$\zeta(2-\zeta)$

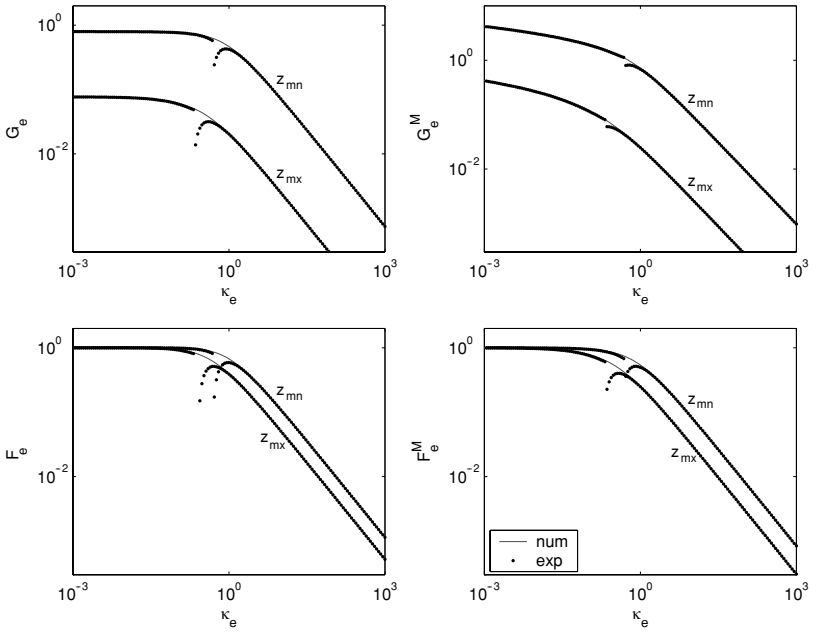

Figure A.1. The electronic functions, computed numerically (full line) and according to the expansions given in the text (dotted line). The curves are labeled with the value of the parameter z, which, for the parameters used in this work, ranges from $z_{\rm mn} = 0.51$ to $z_{\rm mx} = 3.42$. In the range $\min[\frac{1}{2}, 1/(1+z)] < \kappa_{\rm e} < 1$, we have used the expansions valid for $\kappa_{\rm e} > 1$.

https://doi.org/10.1017/S0022377805004009 Published online by Cambridge University Press

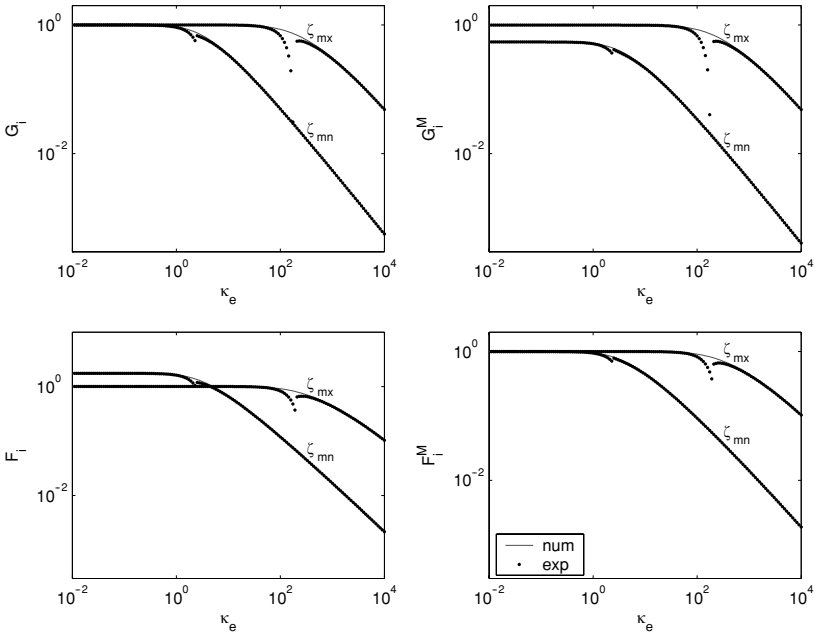

Figure A.2. The ionic functions, computed numerically (full line) and according to the expansions given in the text (dotted line). The curves are labeled with the value of the parameter ζ, being $\zeta_{\rm mn} = 1.32$ and $\zeta_{\rm mx} = 194$. In the range $1 < \kappa_{\rm e} < \max[2, 1 + \zeta]$ we have used the expansions valid for $\kappa_{\rm e} < 1$.

these functions, in a wide range of the parameters z and ζ, except in 'small' regions between, at worst, $\min[\frac{1}{2}, 1/(1 + z)] < \kappa_{\rm e} < 1$ and $1 < \kappa_{\rm e} < \max[2, 1 + \zeta]$ for the electronic and the ionic functions, respectively.

References

[1] Tsytovich, V. N. and de Angelis, U. 1999 *Phys. Plasmas* **6**, 1093.
[2] Tsytovich, V. N. and de Angelis, U. 2000 *Phys. Plasmas* **7**, 554.
[3] Tsytovich, V. N., de Angelis, U. and Bingham, R. 2002 *Phys. Plasmas* **9**, 1079.
[4] Morfill, G. E., Thomas, H., Konopka, U. and Zuzic, M. 1999 *Phys. Plasmas* **6**, 1769.
[5] Shukla, P. K. and Mamun, A. A. 2002 *Introduction to Dusty Plasma Physics*. Bristol: IOP Publishing.
[6] Tsytovich, V. N. and de Angelis, U. 2002 *Phys. Plasmas* **9**, 2497.
[7] Ricci, P., Lapenta, G., de Angelis, U. and Tsytovich, V. N. 2001 *Phys. Plasmas* **8**, 769.

https://doi.org/10.1017/S0022377805004009 Published online by Cambridge University Press